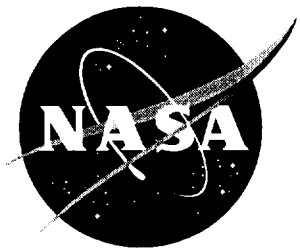

NASA Technical Paper 3663

Low Temperature Mechanical Testing of Carbon-Fiber/Epoxy-Resin Composite Materials

Alan T. Nettles and Emily J. Biss

November 1996

NASA Technical Paper 3663

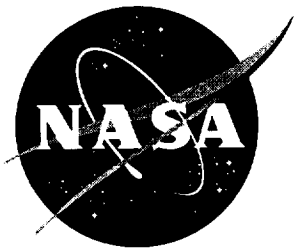

Low Temperature Mechanical Testing of Carbon-Fiber/Epoxy-Resin Composite Materials

Alan T. Nettles and Emily J. Biss
Marshall Space Flight Center • MSFC, Alabama

National Aeronautics and Space Administration
Marshall Space Flight Center • MSFC, Alabama 35812

November 1996

TABLE OF CONTENTS

LIST OF ILLUSTRATIONS

LIST OF TABLES

TECHNICAL PAPER

LOW-TEMPERATURE MECHANICAL TESTING OF CARBON-FIBER/EPOXY-RESIN COMPOSITE MATERIALS

I. INTRODUCTION

Advanced organic matrix, fiber-reinforced composite materials are being increasingly used in the design of aerospace vehicles in order to reduce weight. The benefits of such reduction include increased payload capability, fuel capacity, and reliability through systems redundancy.[1] In order to achieve enhancements in performance, these materials must have a lower density and higher stiffness and strength than conventional materials. They must also display stability over a range of temperatures as well as resistance to damage, moisture absorption, and fatigue. Advanced polymer matrix composites have already been used successfully in a variety of structural applications within the aircraft industry. However, as the use of composite materials expands into the realm of space transportation, these materials are subjected to more hostile environments, including exposure to cryogenic fuels. It is, therefore, important to understand the response of advanced composite materials to such conditions in order to produce a well-designed, structurally sound vehicle using the minimum amount of material. Specifically, the use of cryogenic fuels (liquid oxygen and liquid hydrogen) in current space transportation vehicles, in combination with the proposed use of composite materials in such applications, requires an understanding of how such materials behave at cryogenic temperatures.

The present study has two objectives. The first objective is to examine some of the matrix-dominated properties of carbon-fiber/epoxy-resin systems with an emphasis on temperature dependence. This can be done by using a uniaxial tensile test of a $\pm 45^{\circ}$ laminate that sets up a state of intralaminar shear within the matrix material and causes a matrix controlled failure. The second objective is to explore the effect of temperature on a more realistic manufacturing lay-up in which the fibers are the primary load carrying component. A tensile test on a quasi-isotropic $[+45, 0, -45, 90]_s$ laminate can be used to explore this behavior. Both types of tensile tests were performed on IM7/8551-7 carbon-fiber/epoxy-resin at room, dry ice (CO_2), and liquid nitrogen temperatures. The resulting stress-strain curves were analyzed to obtain an understanding of the effect of temperature on the epoxy matrix as well as on the entire composite. The failed specimens were sectioned and examined using optical and scanning electron microscopy techniques.

In the next section, recent related research efforts are reviewed and relevant results are summarized. The third section provides material preparation details and the experimental procedure adopted in this study. Results obtained are presented in the fourth section and their significance is discussed in the fifth section. Conclusions are then drawn and recommendations are made for future work.

II. BACKGROUND AND LITERATURE REVIEW

Exploring the use of carbon-fiber/epoxy-resin composites in cryogenic applications is not a new concept. The appropriateness of such materials for low temperature applications has been considered for over 20 years. However, it is only fairly recently that more sophisticated carbon-fiber/epoxy-resin materials have been developed and characterized well enough to make them a viable alternative to metallic materials in cryogenic fuel tanks. The properties of these new materials must be explored so that they can be used with confidence and advances can be made in future material development.

There are many facets to material characterization. The mechanical properties of the composite at extreme temperatures must be understood. These include the tensile, compressive, impact, and fatigue

behavior of the material. In addition to the mechanical properties, the thermal and permeability characteristics of the material must also be understood. There is an emerging body of literature exploring the properties of advanced composite materials at cryogenic temperatures, but these properties are far from being completely understood.

Callaghan[2] provides an overview of the basics involved in the use of advanced resin composites in cryogenic applications. He states that, in addition to the material properties listed above, it is important to consider the ease of manufacture and repair when considering candidate materials for low-temperature applications. Often a material will exhibit favorable material properties, but will be too difficult or expensive to manufacture, prohibiting its use.

Callaghan's discussion of structural resins is particularly useful. Resins can be classified as thermosetting, thermoplastic, or a mixture of the two. Each resin system has its advantages and disadvantages. Before curing, thermosetting resins are relatively tacky, flexible, and have a low molecular weight. After curing, the resin transforms into a rigid, high molecular weight material as a result of crosslink formation between polymer chains. A high crosslink density translates into a stiffer matrix as the result of inhibited chain movement. This effect is magnified at lower temperatures. Thermosets are not as tough as a result of their rigid glassy polymer structure. The primary advantages of a thermosetting resin are its stability at elevated temperatures (a high T_g) and its ability to stabilize fibers during compression. The disadvantage is its susceptibility to delamination during low-velocity impact.

Toughened thermosets display an increased toughness while retaining a higher stiffness and T_g. They can be formed in three ways. First, the resin can be chemically altered to reduce the crosslink density. Second, interpenetrating networks (IPN) can be introduced into the matrix. The IPN is a combination of two resin systems at the molecular level that are not covalently bound. The thermoplastic phase of the network provides the resultant matrix with its toughness, while the inclusion of a thermoset in the network results in a high T_g and favorable properties in both high temperature and wet conditions. Third, elastomeric toughening particles can be dispersed throughout the resin. These have the effect of blunting crack growth.

Historically, thermoplastic resins have displayed poor mechanical and physical properties in addition to inferior solvent resistance. Recently, however, advanced thermoplastic resins such as polyetheretherketone (PEEK) have been developed that display more favorable material properties. There is no chemical reaction in the cure cycle of a thermoplast (crosslinks are not formed between polymer backbones). As a result, the matrix displays a high toughness because the polymer chains are able to slide past one another. One of the advantages of thermoplastic resins is their ability to be reprocessed. The primary disadvantage of thermoplasts is the high temperature and pressure required for their curing. Currently, NASA is not considering the use of thermoplastic materials in any of its hardware because of the difficulty and expense of processing. Therefore, toughened thermosets are the most likely candidate for cryogenic applications in the near future.

Kasen provides some of the first definitive literature on the cryogenic material properties of advanced composites.[3] He provides a broad overview of both the static and dynamic mechanical properties of advanced composite materials at cryogenic temperatures. Specifically, he notes that the unidirectional tensile strength of a laminate decreases with decreasing temperature for fibers aligned with the tensile axis and increases for fibers perpendicular to it. He also finds an increase in tensile modulus with decreasing temperature for both configurations. He reports a 50-percent increase in the shear modulus at 77 K (relative to room temperature) from the limited data available.

Ahlborn has done work in the last 10 years examining the static properties of carbon-fiber/epoxy-resin systems, the fatigue behavior of carbon fiber reinforced plastics at cryogenic temperatures,[4] and the cryogenic mechanical response of carbon-fiber reinforced plastics with thermoplastic matrices (PEEK).[5] He assumes the effect of temperature on the fiber is negligible because of its high glass transition temperature (1,700 K). However, he reports that temperature has a significant effect on the properties of rigid (thermosetting), semiflexible (toughened thermosets), and thermoplastic resins. He finds that all three

resins became more brittle with decreasing temperature, which results in decreased fracture strain. However, the thermoplastic resins display a fracture strain of more than twice that of the thermosetting resins and were recommended for future cryogenic applications. In addition, the ultimate tensile strength of all three matrix systems increases with decreasing temperature. He demonstrates that both the matrix strain and strength affect the overall composite behavior. The fracture strain of the entire composite with thermoplastic or toughened thermosetting matrices increased with decreasing temperature. The fracture strain of the composites with thermosetting resins, however, decreased at lower temperatures. Similarly, the ultimate tensile strength of the entire composite with thermoplastic or toughened thermosetting matrices increased with decreasing temperature, while it decreased for those manufactured with thermosetting resins.

Ahlborn has also explored the effect of laminate architecture on stress-strain behavior at 77 K. The unidirectional laminates display the highest stiffness and strength, followed by the cross-ply and then the quasi-isotropic stacking sequences.

From the results of these studies, the following general observations can be made: (1) thermoplastic resins display superior damage tolerance and strength at cryogenic temperatures; however, these benefits are outweighed by the complexity and cost of processing; (2) thermosetting resins are easier and less expensive to manufacture, but have poor damage tolerance and strength at low temperatures; (3) toughened thermosets have been developed to offset some of these problems by combining the superior mechanical properties of thermoplasts with the ease of manufacture of thermosets; and (4) the lay-up of the laminate can significantly affect the mechanical properties of the system, all other variables being equal.

III. EXPERIMENTAL PROCEDURE

A. Material Selection and Preparation

The carbon-fiber/epoxy-resin system used in this study was IM7/8551-7 manufactured by Hercules. The 8551-7 matrix system is a toughened thermoset, which has two distinct phases that separate upon curing. The bulk of the matrix is composed of epoxy which is a highly crosslinked thermoset. The epoxy phase is very rigid and gives the matrix its stiffness. The second phase of the matrix is a low molecular weight thermoplast. The thermoplastic phase is tougher than the epoxy and acts to toughen the overall matrix. Rubberized filler particles are also present between plies. These enhance the toughness between plies. The overall matrix material is considered a thermoset because of the greater percentage of epoxy in the matrix. The glass transition temperature of the entire matrix material as quoted by the manufacturer is 157 °C (315 °F). Representative mechanical properties for the fiber, resin, and the composite are included in table 1.

Table 1. Representative properties for the materials used in this study.

Material	Density* (g/cc)	Tensile Strength (MPa)	Tensile Modulus (GPa)	Tensile Elongation (%)
8551-7 resin	1.28**	99.3	4.09	4.4
IM7 fiber tow***	1.79	3,999	228	1.6
composite****	–	0° = 2,758 90° = 75.8	0° = 159 90° = 8.34	0° = 1.6 90° = 1.0

*All properties based on room temperature, dry conditions.
**Density based on cured resin.
***Filament diameter 5 microns, filament shape round.
****60-percent fiber volume

Composite laminates were made using unidirectional fiber/epoxy mats ("prepreg") laid up in two different configurations. A nine-layer laminate with a stacking sequence of [–45, +45] was produced for the ±45° uniaxial tensile tests (fig. 1).

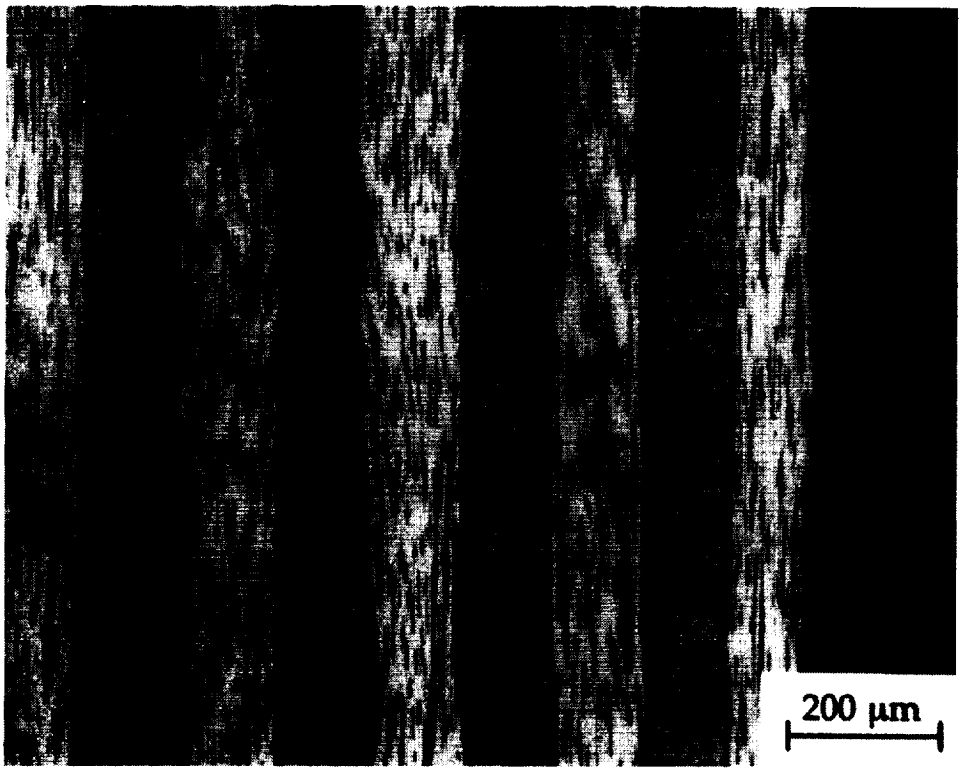

Figure 1. A low magnification cross-sectional photograph of the IM7/8551-7 [±45°] nine-ply laminate. Fibers are running parallel and perpendicular to plane of paper in alternating layers.

A stacking sequence of $[+45, 0, -45, 90]_s$ was used to produce eight-ply laminates for the quasi-isotropic tensile tests. The motivation for these two stacking sequences will be addressed in the next section. The plates were hot-press cured according to the manufacturer's recommendations (appendix). After curing, rectangular test specimens 9-in long by 1-in wide were machined out of the panels. Two strain gauges were affixed to each of the ±45° specimens at 0° and 90° (along and normal to the tensile axis) in order to record the longitudinal and transverse strains. One strain gauge was affixed to each of the quasi-isotropic specimens at 0° in order to record the longitudinal strain. The test specimens were directly gripped during testing.

B. Mechanical Testing

1. ±45° Uniaxial Tensile Testing. In order to have a complete understanding of the ±45° uniaxial tension test, it is first important to clarify the commonly misunderstood difference between intralaminar and interlaminar shear. A laminate can be defined as a material consisting of layers (laminae) bonded together. Interlaminar shear is the shear stress that acts between plies to separate one from another. There are three types of interlaminar shearing stresses: mode I (peeling), mode II (pure shear), and mode III (tearing). These stresses are set up by an out-of-plane load. The interlaminar shear strength is a measure of how strongly the individual plies adhere to each other in the region between plies. Conversely, intralaminar shear is the shear stress that acts within each of the plies. These stresses are set up by in-plane loading. The intralaminar shear strength is a measure of how strongly each individual ply can withstand a given in-plane shear stress.[6]

The first part of the present study is concerned with examining the matrix-dominated properties of carbon-fiber/epoxy-resin composites through the ±45° uniaxial tensile test. In order to isolate the matrix so that it is carrying the applied load instead of the fibers, a state of maximum (pure) shear must be set up within the individual plies. This occurs when the fibers are oriented at 45° to the direction of loading (see the appendix for a detailed discussion). Hence, the ±45° tensile test is also commonly referred to as the intralaminar shear test. Additionally, the plies must be arranged in both the +45° and –45° directions to insure that the laminate is symmetric and that no bending strains are introduced into individual plies when an in-plane tensile load is applied.[6] The ±45° tensile test allows us to measure the intralaminar shear modulus of the specimen by setting up a state of pure shear within each of the plies. In this case, the intralaminar shear modulus is a measure of the resin shear stiffness. The intralaminar shear strength can be measured as well.

The specimens were tested to failure at room (25 °C), dry ice (CO_2, –56.6 °C), and liquid nitrogen (–195.8 °C) temperatures using an Instron testing machine. The width and thickness of each specimen were recorded before testing. The specimens tested at room temperature were simply inserted into the testing apparatus and pulled. For the specimens tested at lower temperatures, an insulated box was constructed to surround the test specimen and hold the dry ice and liquid nitrogen. The speed of the crosshead on all specimens tested was 0.127 cm per minute (0.05 in per minute). As per ASTM standards, the longitudinal and transverse strains were recorded for incremental values of load until strain gauge failure. Values for shear stress and shear strain were then determined using the following equations:

$$\tau^{i}_{12} = P_x^i/2bd \ , \tag{1}$$

$$\gamma^{i}_{12} = \varepsilon_x^i - \varepsilon_y^i \ , \tag{2}$$

where:

P_x^i = load at i^{th} point of ±45° laminate tensile load-deformation curve

τ^{i}_{12} = shear stress at the i^{th} point of the unidirectional shear stress-strain curve

γ^{i}_{12} = shear strain at the i^{th} point of the unidirectional shear stress-strain curve

ε_x^i = longitudinal strain at the i^{th} point of the ±45° laminate tensile load-deformation curve

ε_y^i = transverse strain at the i^{th} point of the ±45° laminate tensile load-deformation curve

b = width of tensile coupon

d = thickness of tensile coupon.[7]

Shear stress versus shear strain was plotted, and the unidirectional shear modulus of the lamina was determined by using the following equation:

$$G_{12} = \Delta\tau_{12}/\Delta\gamma_{12} \tag{3}$$

where:

G_{12} = shear modulus of lamina

$\Delta\tau_{12}/\Delta\gamma_{12}$ = slope of the plot of the unidirectional shear stress-shear strain curve within the linear portion of the curve.[7]

The lamina shear strength was calculated using the following equation:

$$S = P/2bd \ , \tag{4}$$

where:

S = ultimate lamina shear strength

P = maximum load on ±45° laminate tensile load-deformation curve

b = width of tensile coupon

d = thickness of tensile coupon.[7]

2. Quasi-Isotropic Uniaxial Tensile Testing. The second part of the present study is concerned with exploring the effects of temperature on a lay-up more commonly used for industrial applications. The ±45° lay-up used in the first section of this study was necessary in order to isolate the matrix as the primary load-carrying component of the composite. However, it is precisely for this reason that such a lay-up would never be used in product manufacture. The effectiveness of composite materials is the result of a judicious combination of material properties from two or more constituent phases. In this case, the fibers are extremely strong, which permits them to carry high loads. However, they are also very brittle, which allows them to be easily damaged and compromises their load-carrying capability. The matrix, which is relatively ductile yet not very strong, is introduced to protect the fibers, to provide a means of connecting them, and to transfer the applied load to the fibers.

The quasi-isotropic specimens were tested at room, dry ice (CO_2), and liquid nitrogen temperatures as outlined in the previous section. The speed of the crosshead was once again 0.127 cm per minute (0.05 in per minute). The longitudinal strain was recorded for incremental values of load, and the stress was determined using the following equation:

$$\sigma_x^i = P_x^i/bd \ , \tag{5}$$

where:

P_x^i = load at i^{th} point of quasi-isotropic laminate tensile load-deformation curve

σ_x^i = tensile stress at the i^{th} point of the unidirectional tensile stress-strain curve

b = width of tensile coupon

d = thickness of tensile coupon.

Tensile stress versus tensile strain was plotted and the lamina tensile modulus was determined by using the following equation:

$$E = \Delta\sigma/\Delta\varepsilon \ , \tag{6}$$

where:

E = tensile modulus of unidirectional composite

$\Delta\sigma/\Delta\varepsilon$ = slope of the plot of the unidirectional tensile stress-tensile strain curve within the linear portion of the curve.

The tensile strength of the specimen was determined using the following equation:

$$TS = P/bd \ , \tag{7}$$

where:

TS = ultimate unidirectional tensile strength

P = maximum load on quasi-isotropic laminate tensile load-deformation curve

b = width of tensile coupon

d = thickness of tensile coupon.

C. Post Deformation Microstructure

In order to obtain a better understanding of the material behavior, specimen sections were examined using optical and scanning electron microscopes. The ±45° specimens were selected for examination. First, the outer edges of the gauge section of the specimens tested at room temperature, dry ice (CO_2) and LN_2 (i.e., in the thickness plane), were examined optically at low magnification. Second, sections were cut parallel to the fiber orientation (i.e., +45° or –45° to the tensile axis) from the grip section and the gauge section below the fracture region in the specimens failed at room temperature, and from the gauge section in the specimen failed at LN_2. These specimens were spring-clamped, mounted, and polished prior to examination. They were then examined with optical and scanning electron microscopes.

IV. RESULTS

A. Mechanical Testing

1. ±45° Uniaxial Tensile Testing. Using the procedure outlined in the previous section, shear stress-shear strain curves were generated for each of the ±45° samples tested. From these curves, the shear modulus of each specimen was determined, and the average shear modulus for all of the specimens tested at a given temperature was calculated. In addition, the shear stress at fracture (shear strength) and the average shear strength for all of the specimens tested at a given temperature were calculated. It is relevant to emphasize that in all cases, strain gauges failed prior to the specimen and, therefore, strain data were not obtained for the entire duration of the test.

The shear stress-shear strain curves generated from the samples tested at room temperature are initially linear and rapidly become nonlinear (fig. 2). The average shear modulus of the specimens tested at room temperature was 5.6 GPa with a standard deviation of 0.4 GPa. The average shear strength was 94 MPa with a standard deviation of 5.4 MPa (table 2).

The shear stress-shear strain curves generated from the samples tested at CO_2 are initially linear and remain so to higher stress levels than those from the room temperature tests, but eventually transition into a nonlinear region as well (fig. 2). The average shear modulus of the specimens tested at CO_2 was 6.8 GPa. The average shear strength was 107.9 MPa (table 2). There were four [±45°] specimens tested at CO_2 (three until failure) and, therefore, a meaningful standard deviation for the modulus and shear strength could not be calculated. In order to get an indication of the spread, the values calculated for each specimen are reported (table 2).

The shear stress-shear strain curves generated from the samples tested at LN_2 are entirely linear (fig. 2). The average shear modulus of the specimens tested at LN_2 was 8.1 GPa with a standard deviation of 0.2 GPa. The average shear strength was 102 MPa with a standard deviation of 4.3 MPa (table 2).

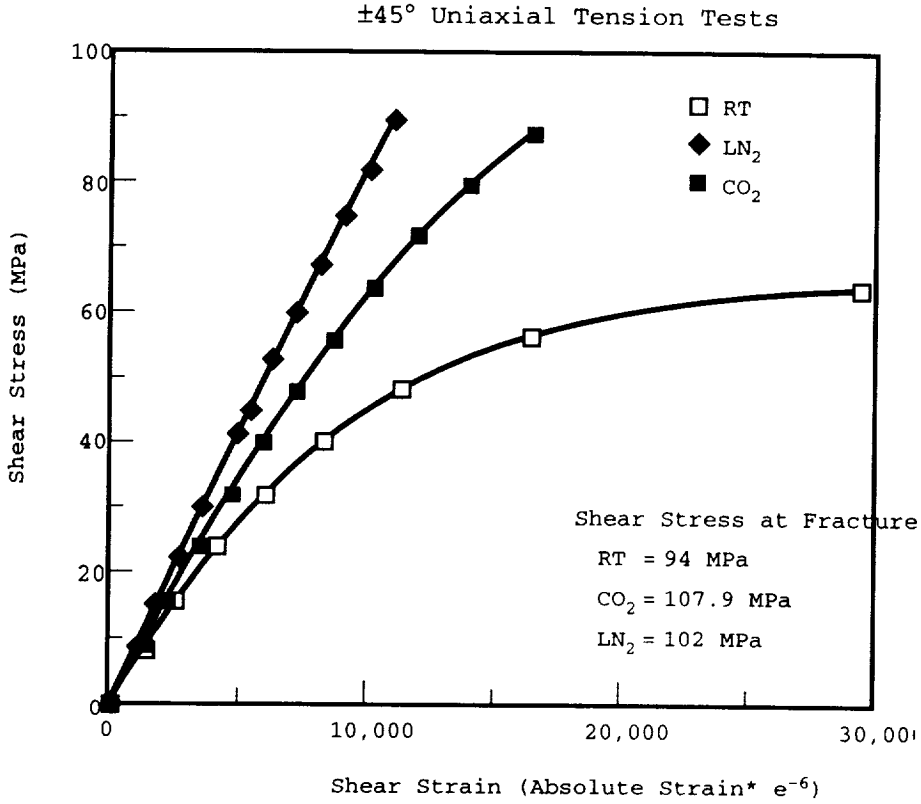

Figure 2. Shear stress-shear strain curves of [±45°] specimens tested at room temperature, dry ice (CO_2), and in LN_2.

Table 2. Mechanical properties of the [±45°] laminate.

Temperature	Average Shear Modulus (GPa)	Standard Deviation (GPa)	Average Shear Strength (MPa)	Standard Deviation (MPa)
room temperature	5.6	0.4	94	5.4
carbon dioxide	6.8	[7.0, 7.0, 6.3, 6.7]*	107.9	[109.9, 102.9, 110.8]*
liquid nitrogen	8.1	0.2	102	4.3

*Meaningful standard deviation not available in trials with four specimens or less, actual measurements given.

2. Quasi-Isotropic Uniaxial Tensile Testing. Using the procedure outlined in the previous section, tensile stress-strain curves were generated for each of the quasi-isotropic samples tested. From these curves, the tensile modulus of each specimen was determined, and the average tensile modulus for all of the specimens tested at a given temperature was calculated. In addition, the tensile strength was computed, and the average tensile strength for all of the specimens tested at a given temperature was calculated. There were only two or three quasi-isotropic specimens tested at each of the three temperatures and, therefore, a meaningful standard deviation for the modulus and tensile strength could not be calculated. In order to get an indication of the spread, the values calculated for each specimen are reported (table 3).

The tensile stress-strain curves generated from the samples tested at room temperature are linear (fig. 3). The tensile modulus of the specimens tested at room temperature was 61.7 GPa. The average tensile strength was 761.9 MPa (table 3).

Table 3. Mechanical properties of the quasi-isotropic laminate.

Temperature	Average Tensile Modulus (GPa)	Standard Deviation (GPa)	Average Tensile Strength (MPa)	Standard Deviation (MPa)
room temperature	61.7	[61.9, 61.4, 61.7]*	761.9	[726, 798.9, 760.8]*
carbon dioxide	61.1	[63.6, 58.5]*	808.2	[804.1, 812.3]*
liquid nitrogen	64.4	[66.7, 60.8, 65.6]*	694.84	[659, 695.2, 730.2]*

*Meaningful standard deviation not available in trials with three specimens or less, values for each specimen given.

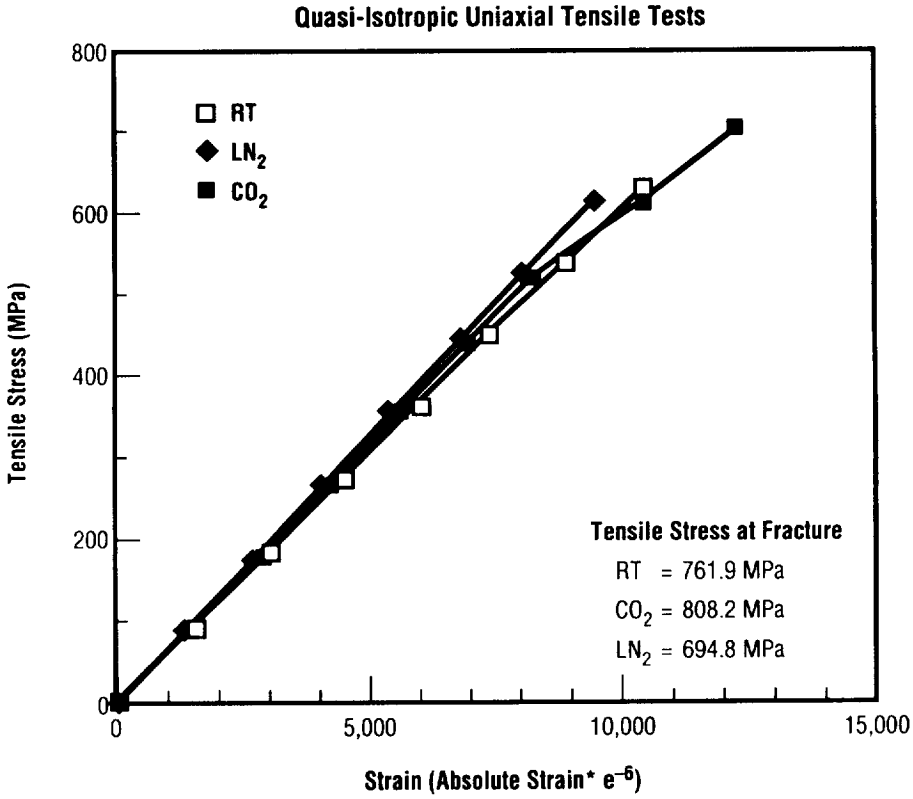

Figure 3. Tensile stress-strain curves of quasi-isotropic specimens tested at room temperature, dry ice (CO_2), and LN_2.

The tensile stress-strain curves generated from the samples tested at CO_2 are linear as well (fig. 3). The average tensile modulus of the specimens tested at CO_2 was 61.1 GPa. The average tensile strength was 808.2 MPa (table 3).

The tensile stress-strain curves generated from the samples tested at LN_2 are also linear (fig. 3). The average tensile modulus of the specimens tested at LN_2 was 64.4 GPa. The average tensile strength was 694.8 MPa (table 3).

B. Post Deformation Microscopy

Optical microscopy techniques were used to evaluate the deformation features and fracture characteristics of the ±45° uniaxial tensile specimens. It was anticipated that these specimens, by virtue of a matrix-dominated failure mode, would provide valuable insight into failure mechanisms that are likely operative at each of the test temperatures.

The edge section along the gauge length of the unpolished specimens was initially examined optically at a relatively low magnification. Figures 4a to 4c show an area of the specimens near the fracture surface following tensile tests at room, dry ice (CO_2), and LN_2 temperatures, respectively. It can be seen that the specimen tested at room temperature shows extensive microcracking in each of the plies, while the specimen tested at CO_2 displays less microcracking, and the specimen tested at LN_2 virtually none. The edge of each specimen was subsequently examined at locations away from the fracture surface. It was found that the features observed near the fracture region (figs. 4a to 4c) were consistently noted along the length of each specimen (figs. 5a to 5c).

The mounted and polished specimen cross sections were then examined at higher magnifications in order to determine the effect of temperature on fracture propagation and damage resistance at a microstructural level. Features of interest included an examination of the fiber-matrix interface for any evidence of debonding and the likelihood of observing extensive microcracks in the entire cross section, consistent with those observed on the surface (figs. 4a to 4c and 5a to 5c). Two specimens, one from the gauge section and the other from the grip section of a [±45°] specimen tested at room temperature, were examined. The specimen from the grip section shows no evidence of microcracks within each of the individual plies (fig. 6a) whereas microcracks are interspersed in the specimen extracted from the gauge section (fig. 6b). The specimen from the gauge section was next examined at high magnification. A representative micrograph is shown in figure 7. From figure 6b and figure 7, it is evident that these microcracks are solely in the matrix. From these two figures, we also conclude that the section we cut from the specimen is not exactly parallel to one set of fibers and therefore, the observed crack in figure 7 actually is not in the plane of the paper, but intersects it at a shallow angle.

The microstructure of the cross-section of a specimen tested in LN_2 is shown in figure 8 for purposes of comparison with figure 6b. Almost no microcracks are present consistent with the low magnification observation of the specimen edge (figs. 4c and 5c).

Finally, the fiber-matrix interface in three specimens (an undamaged specimen, one tested at room temperature, and one tested at LN_2) were examined at high magnification to identify possible fiber-matrix debonding. The results, shown in figures 9a to 9c, demonstrate that no substantial fiber-matrix debonding had occurred in any of the specimens.

V. DISCUSSION

A. ±45° Uniaxial Tensile Testing

The experimental results presented in the previous section, in combination with the known material properties of the 8551-7 resin system, can now be used to describe some forms of matrix behavior as a function of temperature.

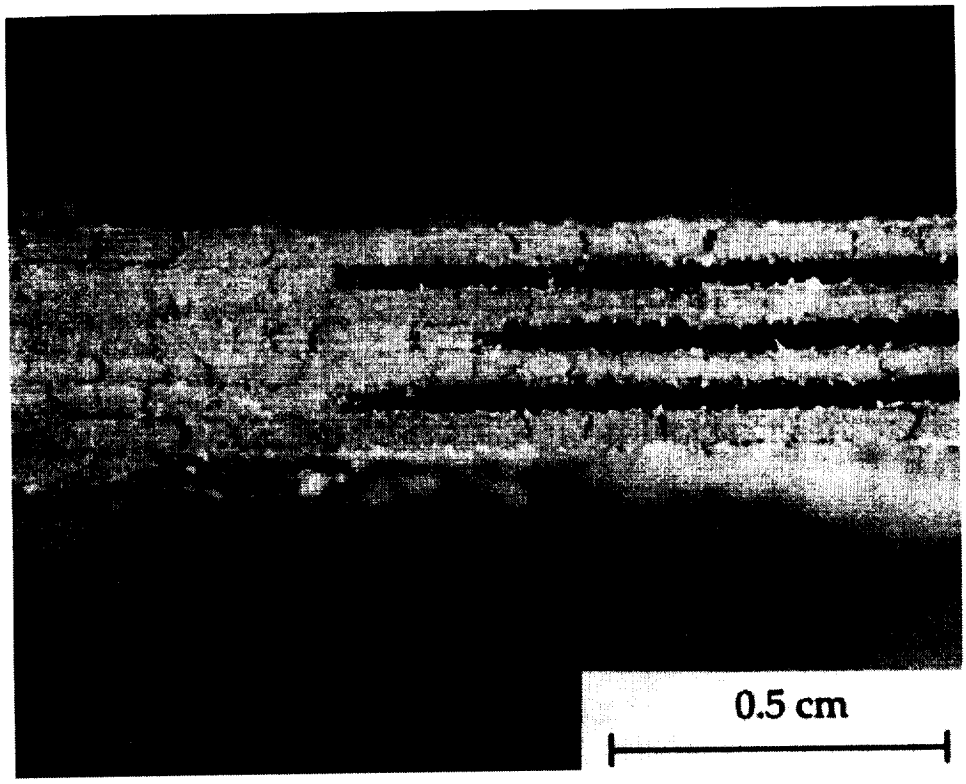

Figure 4a. An edge-view near the fracture surface of [±45°] tensile specimen tested at room temperature.

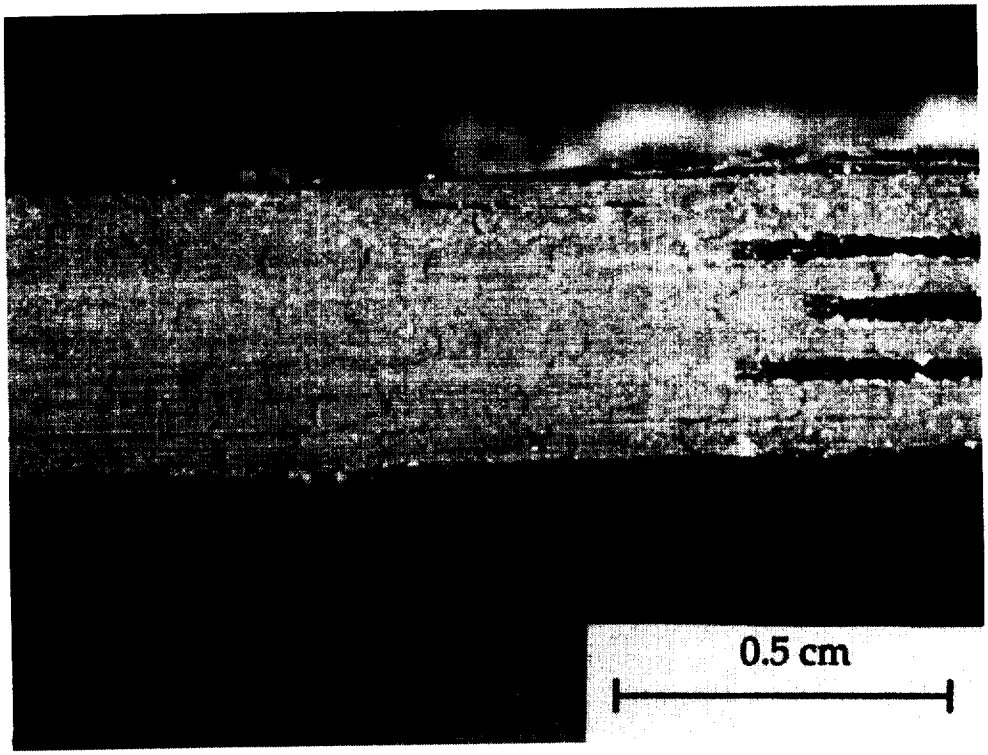

Figure 4b. An edge-view near the fracture surface of [±45°] tensile specimen tested in dry ice (CO_2).

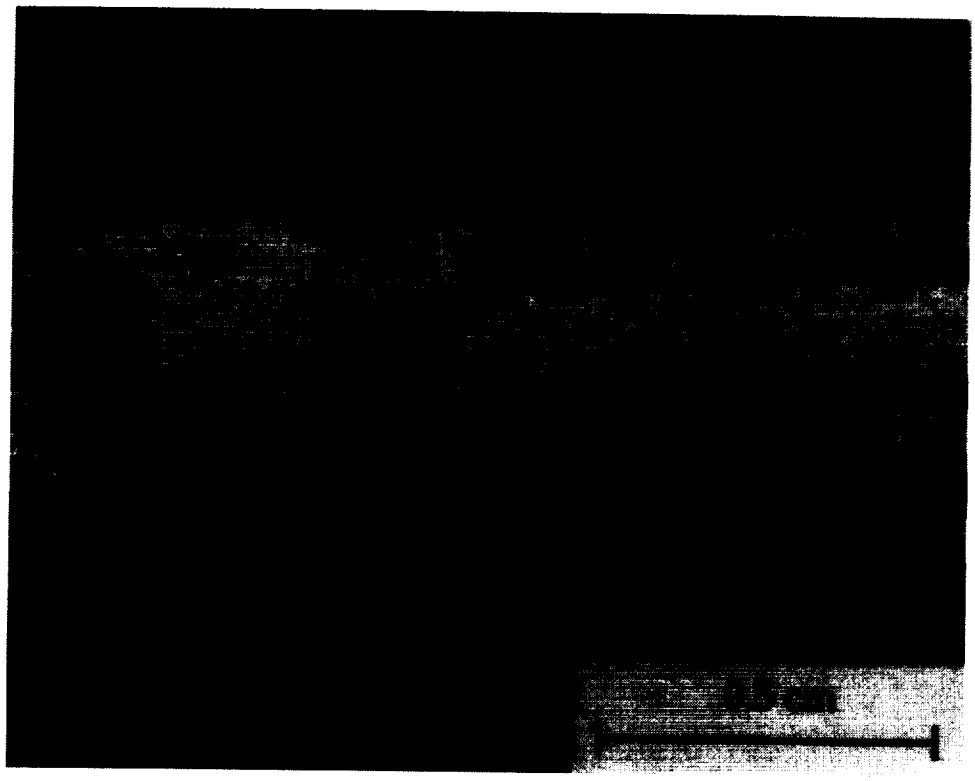

Figure 4c. An edge-view near the fracture surface of [±45°] tensile specimen tested in LN_2.

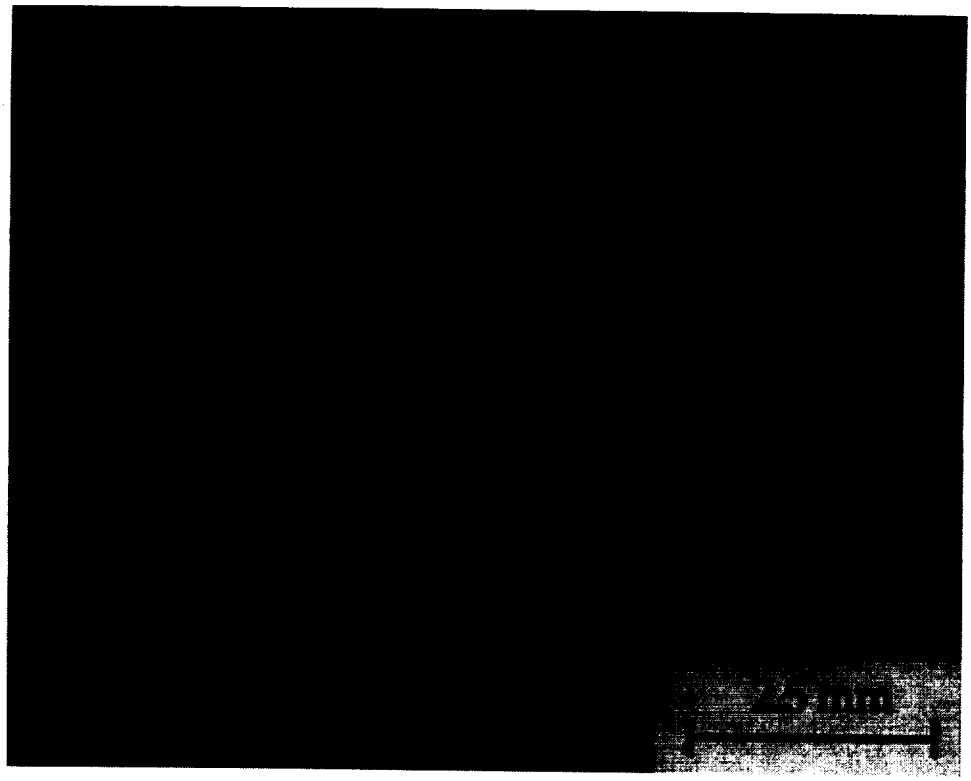

Figure 5a. An edge-view along the gauge length away from the fracture surface of [±45°] tensile specimen tested at room temperature.

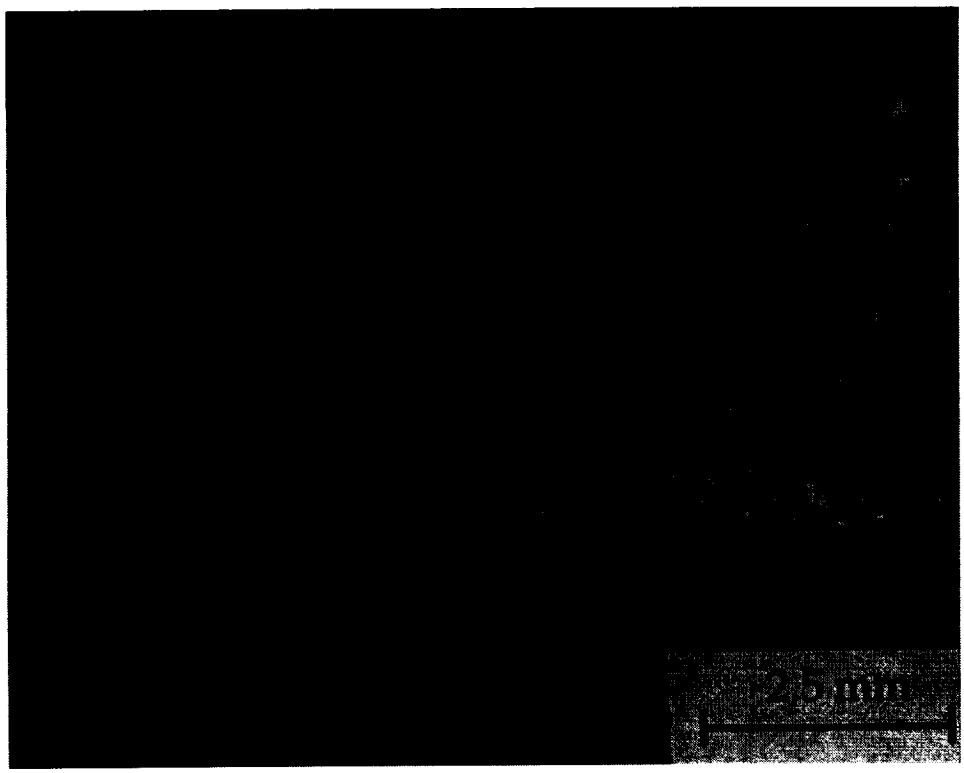

Figure 5b. An edge-view along the gauge length away from the fracture surface of [±45°] tensile specimen tested in dry ice (CO_2).

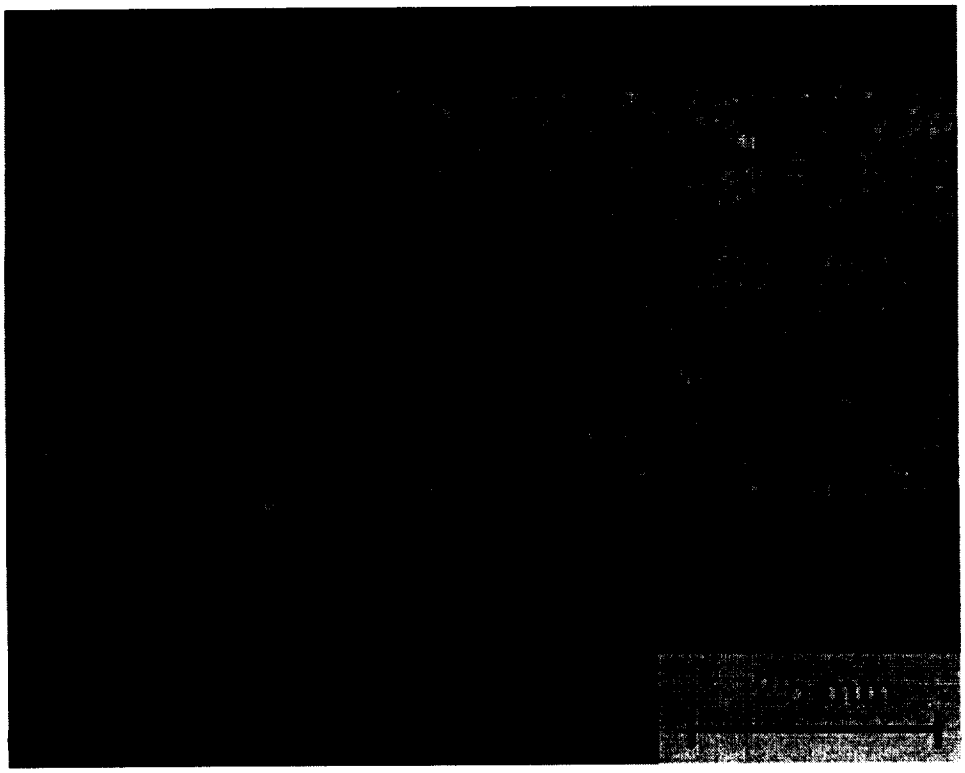

Figure 5c. An edge-view along the gauge length away from the fracture surface of [±45°] tensile specimen tested in LN_2.

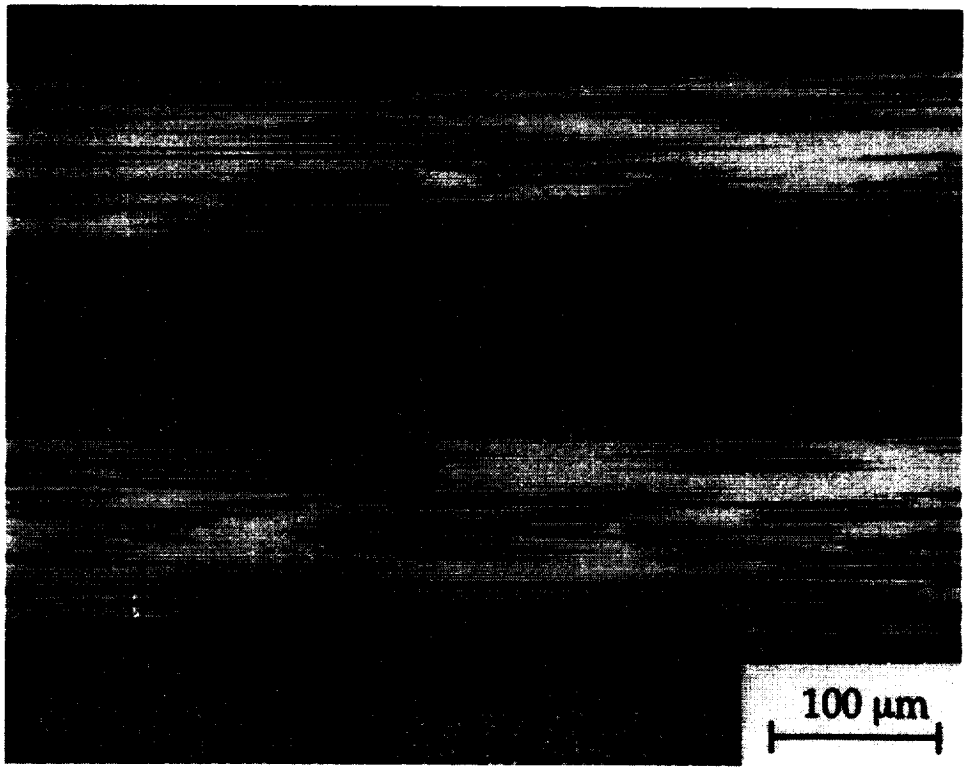

Figure 6a. A polished cross section of the [±45°] room temperature specimen with fibers running parallel and perpendicular to plane of paper from specimen grip section.

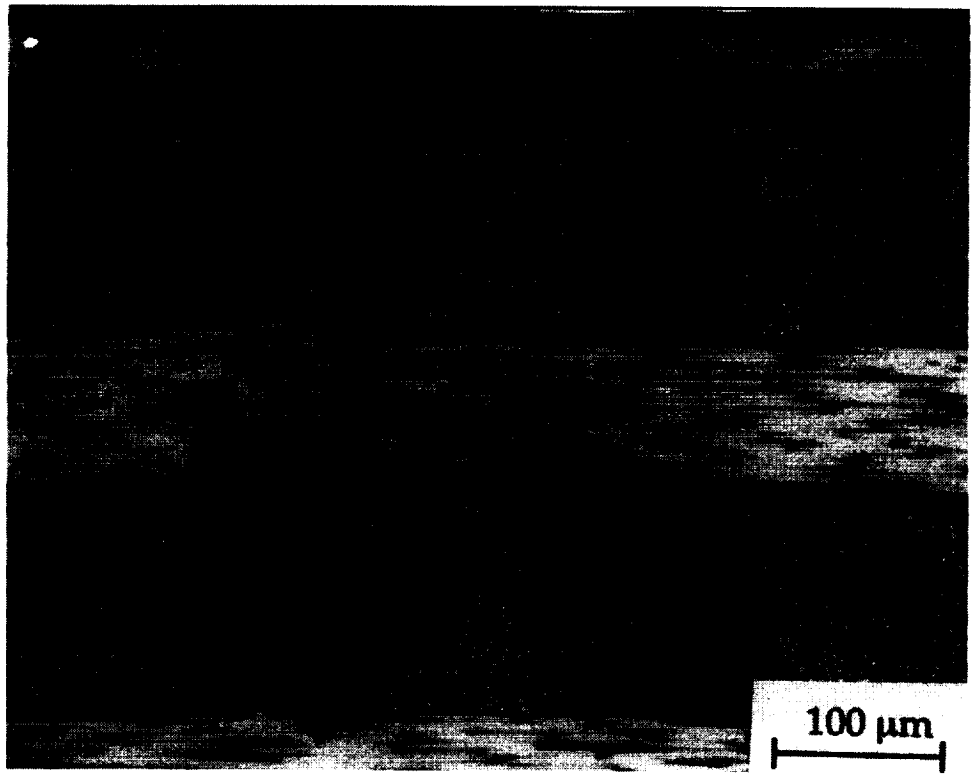

Figure 6b. A polished cross section of the [±45°] room temperature specimen with fibers running parallel and perpendicular to plane of paper from specimen gauge section.

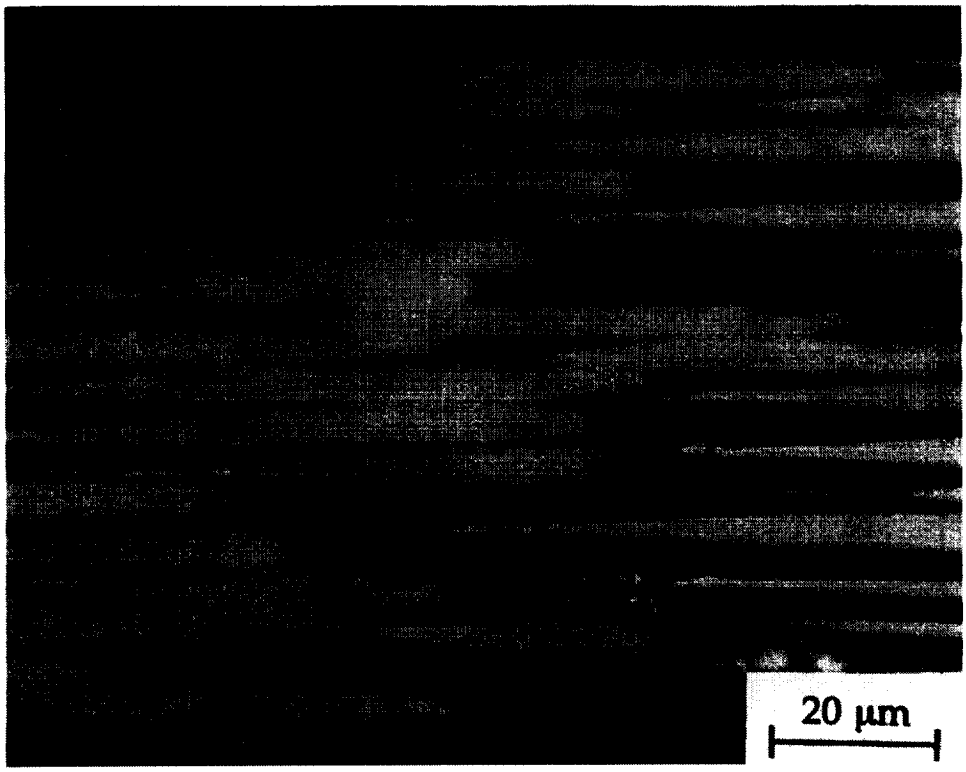

Figure 7. A high-magnification micrograph showing a crack advancing between fibers that are almost parallel to plane of paper in a [±45°] room-temperature specimen.

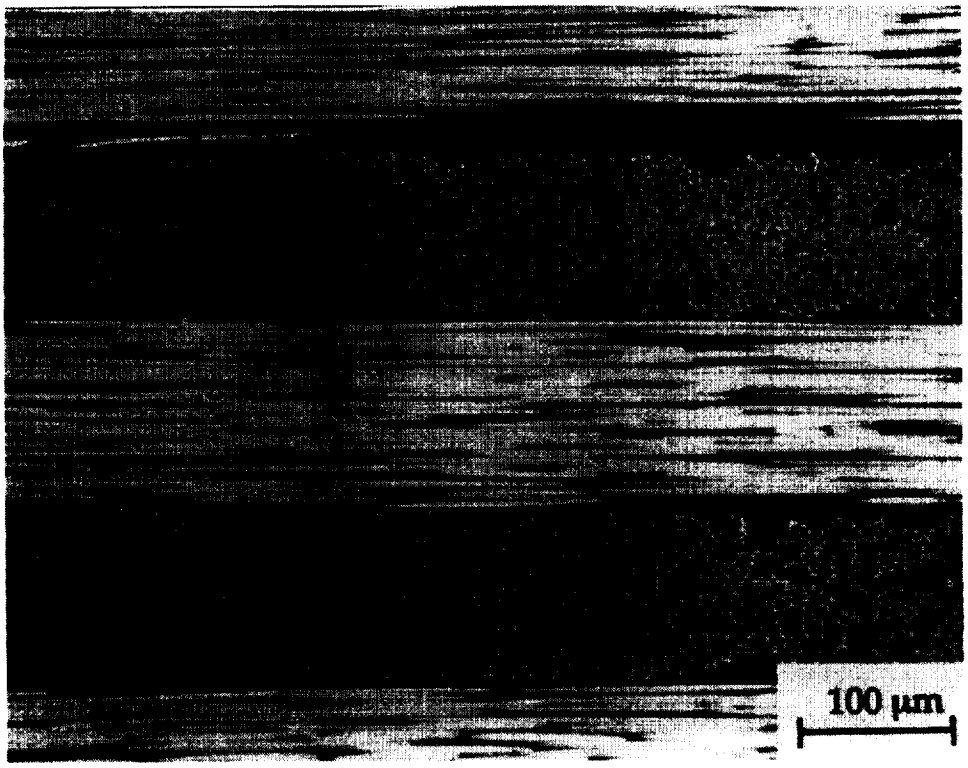

Figure 8. A polished cross section of the gauge section of a [±45°] specimen showing the absence of significant microcracks. Fibers are running parallel and perpendicular to plane of paper.

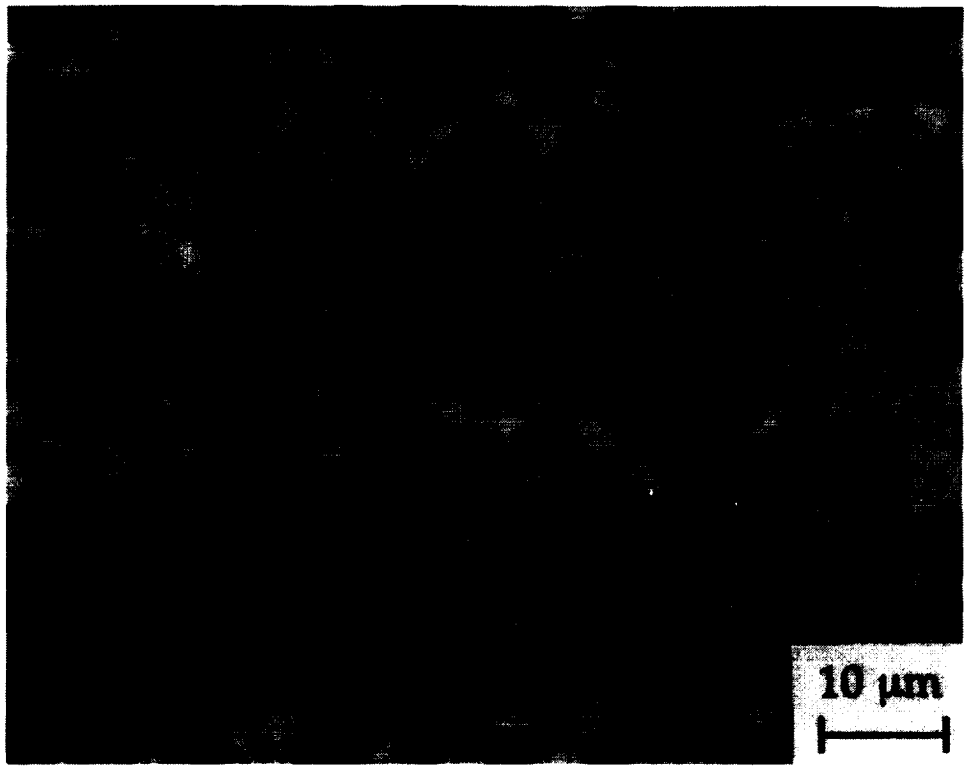

Figure 9a. The absence of obvious matrix-fiber debonding in [±45°] specimens; grip section of room-temperature specimen.

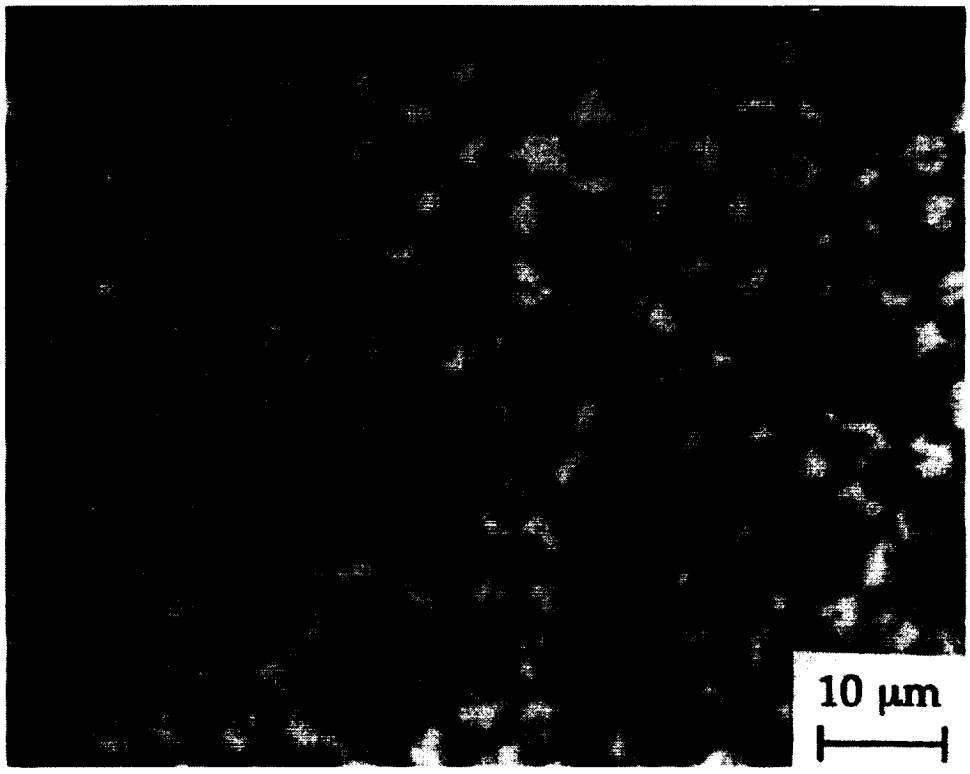

Figure 9b. The absence of obvious matrix-fiber debonding in [±45°] specimens; gauge section of room-temperature specimen.

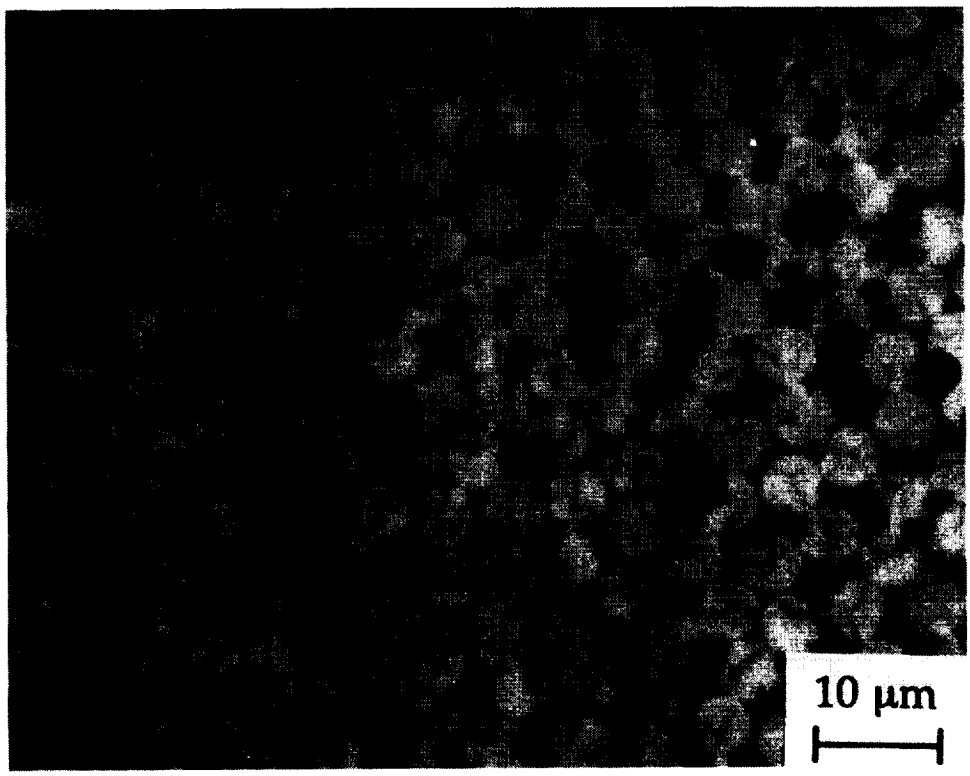

Figure 9c. The absence of obvious matrix-fiber debonding in [±45°] specimens; gauge section of LN_2 specimen.

The deformation mechanisms operating within the matrix are found to be highly temperature dependent. This is evidenced in two ways: first, by the shape of the shear stress-shear strain curves; and second, by what is observed in the microscopic analysis.

For metallic materials, the linear region of the stress-strain curve corresponds to elastic deformation and the nonlinear region to plastic deformation. However, when working with noncrystalline substances (such as epoxy), the glass transition temperature (T_g) determines whether a material can exhibit viscous, or non-linear, behavior. Below the glass transition temperature a noncrystalline material is considered an amorphous solid, above it a rubbery solid and, as the temperature increases, a viscous liquid.[8] A noncrystalline material such as a polymer can only exhibit viscous behavior above T_g; below T_g, the material will fail before it plastically deforms.

All of the tests in the current study were conducted well below T_g for the epoxy resin (157 °C). This indicates that the nonlinear regions of the shear stress-shear strain curves generated by the tests at room temperature and in dry ice are not the result of viscous, or plastic, deformation (fig. 2). This nonlinear behavior is thought to be the result of microcrack accumulation throughout the matrix. The extensive nonlinear region displayed in the room temperature stress-strain curves would correspond to a high density of microcracks throughout the material (fig. 2). The more limited nonlinear region in the curves generated from the tests done in dry ice and the exclusively linear behavior of the stress-strain curves generated from the specimens tested in LN_2 imply that there is a progressive decrease in microcrack accumulation within the specimen with decreasing temperature. Strain gauge failure occurred prior to specimen failure in all cases; however, strain gauges on two out of the six specimens tested in LN_2 remained functional to within 444.8 N (100 lb) of the load at specimen failure, and the stress-strain curves generated from these tests were consistent with the others (i.e., entirely linear). Therefore, it was hypothesized that there would be no substantial nonlinear behavior in the specimens tested at LN_2, which implies minimal microcracking prior to failure.

The hypothesis outlined above was confirmed through the use of optical microscopy. It can be seen that the specimens tested at room temperature show extensive microcracking both on the surface (figs. 4a and 5a) and in the interior of the test specimens (figs. 6b and 7). The specimens tested in dry ice display less microcracking on the surface (figs. 4b and 5b) than the specimens tested at room temperature, and the specimens tested in LN_2 display almost no microcracking both on the surface (figs. 4c and 5c) and in the interior (fig. 8). Therefore, it can be concluded that microcracking is the source of the nonlinear stress-strain behavior observed, and the formation of microcracks within the matrix is clearly inhibited as temperature decreases. This is because the material constituents become more brittle as temperature decreases and are less able to blunt cracks. These cracks are allowed to grow and ultimately result in specimen failure.

A mechanical property that is sensitive to the deformation characteristics of the matrix is toughness. Toughness can be defined as a measure of the ability of a material to absorb energy up to fracture.[9] The formation and growth of microcracks is one such mechanism of energy absorption. Therefore, a decrease in microcracking with decreasing temperature corresponds to a decrease in matrix toughness with decreasing temperature; the matrix is unable to absorb as much energy before complete specimen failure at low temperatures as it is at higher temperatures. It is important to note, however, that specimen failure can also be defined as the onset of microcracking (as opposed to complete specimen failure), in which case the specimens tested at cryogenic temperatures would be tougher than the ones tested at room temperature.

As expected, there is a modest increase in matrix stiffness as temperature decreases. The average shear moduli increase from 5.6 GPa at room temperature to 8.1 GPa at LN_2. This is because as temperature decreases the motion of atoms in the side groups of the main polymeric chains is inhibited.

There is no clear correlation between the shear strength of the matrix and temperature. The average shear strength is 94 MPa at room temperature, increases to 107.9 MPa in dry ice (CO_2), and then decreases slightly to 102 MPa in LN_2. It appears that the trend is toward increased shear strength with decreasing temperature. However, the inconsistent jump of shear strength in dry ice (CO_2) remains anomalous and warrants further investigation.

Temperature does not affect the ability of the matrix to transfer the applied load to the fibers. As expected, there is no obvious evidence of fiber-matrix debonding in the sample taken from the grip section of a specimen tested at room temperature (in other words a sample subjected to no loading) (fig. 9a). Additionally, there is no evidence of fiber-matrix debonding in the specimens tested at room temperature (fig. 9b) and in LN_2 (fig. 9c). The integrity of the fiber-matrix bond is, therefore, temperature independent, within the range of conditions evaluated in this effort.

B. Quasi-Isotropic Uniaxial Tensile Testing

Again, the experimental results discussed in the previous section, in combination with the known material properties of the IM7/8551-7 system, are used to characterize the behavior of the fiber-resin system as a function of temperature. The tensile stress-tensile strain curves generated by the quasi-isotropic tests were linear in all three cases; this is indicative of the dominant role of the fiber in this configuration. Likewise, the absence of significant variation in properties such as modulus and strength can be attributed to the insensitivity of the fiber properties to temperature within the range of temperatures examined (fig. 3). It cannot be assumed that the quasi-isotropic specimens accumulate a significant amount of microcracks before strain gauge failure because specimen failure is fiber dominated and microcrack accumulation within the matrix would not necessarily result in nonlinear stress-strain behavior. As with the $\pm 45^\circ$ tensile tests, strain gauge failure occurred before specimen failure, and it is impossible to know if the stress-strain curves remained linear for the duration of the test. However, most of the strain gauges failed within no more than 889.6 N (200 lb) of the maximum loading and, therefore, it is assumed that the curves remained substantially linear until specimen failure. The existence or absence of microcracks within the quasi-isotropic specimens was not verified visually. Such corroboration is suggested for future efforts.

Because the presence of microcracks at room, dry ice (CO_2), and liquid nitrogen temperatures was not established, the toughness of the quasi-isotropic specimens (as defined in the previous section) cannot be compared.

The average moduli for the specimens tested at room, dry ice, and liquid nitrogen temperatures are 61.7, 61.1, and 64.4 GPa, respectively (table 3), which is well within the range of experimental error. Therefore, it can be concluded that temperature has no appreciable affect on the modulus within the range of temperatures tested. Again, this is an area which warrants further inquiry.

Finally, the tensile strength of the quasi-isotropic specimens appears to show no obvious systematic variation with temperature. In fact, even at a given temperature, extensive scatter in data is apparent (table 3). The strength levels are very high, however, varying from six to eight times those observed for the [±45°] laminate. This clearly indicates the dominant role of the fibers and a possible reason for the scatter in data that may be related to intrinsic flaws in the fibers.

VI. CONCLUSION

The matrix dominated properties of carbon-fiber/epoxy-resin systems have been explored as a function of temperature in the present study. In addition, the effect of temperature on a more realistic quasi-isotropic manufacturing lay-up was investigated. It was found that the formation of microcracks within the matrix was clearly inhibited at lower temperatures, which corresponds to a decrease in toughness. As expected, a modest increase in matrix stiffness was observed with a decrease in temperature. There was a marginal increase in matrix strength with decreasing temperatures, and temperature did not appear to affect the ability of the matrix to transfer the applied load to the fibers.

Because the response to a uniaxial applied stress in quasi-isotropic specimens is fiber dominated, the stress-strain curves generated from these specimens cannot be used to determine whether or not microcracks accumulate within the matrix at each of the temperatures tested. As a result, the toughness at each temperature could not be compared. Temperature has no statistically significant effect on the tensile modulus. The average tensile strength showed no systematic variation with temperature and, because of the large scatter in data, the reason for this behavior remains unclear.

VII. RECOMMENDATIONS FOR FUTURE WORK

The matrix behavior as a function of temperature was well characterized in the present effort. However, the results suggest the need for further investigation in several areas. First, because the formation of microcracks within the matrix has significant implications for the permeability of the material, further investigation into the causes of the observed decrease in microcracking with decreasing temperatures is advised. Second, the effect of temperature on the shear strength of the matrix needs to be established in greater detail.

The tests done on the quasi-isotropic specimens were largely a preliminary step in what needs to be a more extensive study in order to understand the effect of temperature on a realistic stacking sequence. First, microscopy techniques should be employed in order to determine the existence or absence of microcracking within the matrix. Additional testing is also desirable to more fully understand the inconsistencies observed in the tensile modulus and strength measured.

REFERENCES

1. McCullough, R.L.: "Concepts of Fiber-Resin Composites." Marcel Dekker, Inc., New York, 1971, p. 12.

2. Callaghan, M.T.: "Cryogenics," vol. 31, 1991, pp. 282–287.

3. Kasen, M.B.: "Cryogenics," vol. 15, 1975, pp. 701–722.

4. Ahlborn, K.: "Cryogenics," vol. 28, 1988, pp. 267–672.

5. Ahlborn, K.: "Cryogenics," vol. 31, 1991, pp. 252– 256.

6. Nettles, A.T.: NASA TM 108495, Marshall Space Flight Center, 1995.

7. "Standard Practice for In-Plane Shear Stress-Strain Response of Unidirectional Polymer Matrix Composites," D 3518/D 3518M-91.

8. Callister Jr., W. D.: "Materials Science and Engineering: An Introduction." Third edition, John Wiley & Sons, Inc., New York, 1994, p. 480.

9. Ibid, p. 124.

APPENDIX

Consider the total stress/strain relationship matrix form:

$$\begin{bmatrix} \varepsilon_x \\ \varepsilon_y \\ \varepsilon_{xy} \end{bmatrix} = \begin{bmatrix} \overline{S_{11}}\,\overline{S_{12}}\,\overline{S_{16}} \\ \overline{S_{12}}\,\overline{S_{22}}\,\overline{S_{26}} \\ \overline{S_{16}}\,\overline{S_{26}}\,\overline{S_{66}} \end{bmatrix} \begin{bmatrix} \sigma_x \\ \sigma_y \\ \tau_{xy} \end{bmatrix}, \tag{A-1}$$

where,

$$\begin{aligned}
\overline{S_{11}} &= S_{11}\cos^4\theta + (2S_{12} + S_{66})\cos^2\theta\sin^2\theta + S_{22}\sin^4\theta, \\
\overline{S_{12}} &= (S_{11} + S_{22} - S_{66})\cos^2\theta\sin^2\theta + S_{12}(\cos^4\theta\sin^4\theta), \\
\overline{S_{22}} &= S_{11}\sin^4\theta + (2S_{12} + S_{66})\cos^2\theta\sin^2\theta + S_{22}\cos^4\theta, \\
\overline{S_{16}} &= (2S_{11} - 2S_{12} - S_{66})\cos^3\theta\sin\theta + (2S_{12} - 2S_{22} + S_{66})\cos\theta\sin^3\theta, \\
\overline{S_{26}} &= (2S_{11} - 2S_{12} - S_{66})\cos\theta\sin^3\theta + (2S_{12} - 2S_{22} + S_{66})\cos^3\theta\sin\theta, \\
\overline{S_{66}} &= (2S_{11} + 2S_{22} - 4S_{12} - S_{66})\cos^2\theta\sin^2\theta + S_{66}/2(\cos^4\theta + \sin^4\theta),
\end{aligned} \tag{A-2}$$

and the S_{ij} are determined from the lamina engineering constants as:

$$\begin{aligned}
S_{11} &= \frac{1}{E_1}, \qquad S_{22} = \frac{1}{E_2}, \\
S_{12} &= \frac{-\upsilon_{12}}{E_1}, \qquad S_{66} = \frac{1}{G_{12}}.
\end{aligned} \tag{A-3}$$

Referring back to equation (A-1) and applying only a tensile load in the x-direction, the strain/stress relationship for a lamina becomes:

$$\begin{bmatrix} \varepsilon_x \\ \varepsilon_y \\ \varepsilon_{xy} \end{bmatrix} = \begin{bmatrix} \overline{S_{11}}\,\overline{S_{12}}\,\overline{S_{16}} \\ \overline{S_{12}}\,\overline{S_{22}}\,\overline{S_{26}} \\ \overline{S_{16}}\,\overline{S_{26}}\,\overline{S_{66}} \end{bmatrix} \begin{bmatrix} \sigma_x \\ 0 \\ 0 \end{bmatrix}. \tag{A-4}$$

Thus,

$$\varepsilon_{xy} = \overline{S_{16}}\sigma_x, \tag{A-5}$$

and if θ is not either 0° or 90°, then the x-direction tensile stress will cause an x-y plane shear strain. In order to maximize this x-y shear strain, $\overline{S_{16}}$ must be maximized. From equation (A-2):

$$\overline{S_{16}} = (2S_{11} - 2S_{12} - S_{66})\cos^3\theta\sin\theta + (2S_{12} - 2S_{22} + S_{66})\cos\theta\sin^3\theta.$$

which will be $\frac{\partial\overline{S_{16}}}{\partial\theta} = 0$, which occurs at $\theta = \pm 45°$.

All of the above analysis is based on the assumption of constant stress being applied across the specimen's edges. As was shown, this type of applied stress will result in a shear strain (given by equation (A-5)). Figure A-1 shows the deformation that a 45° ply will assume given this uniform stress.

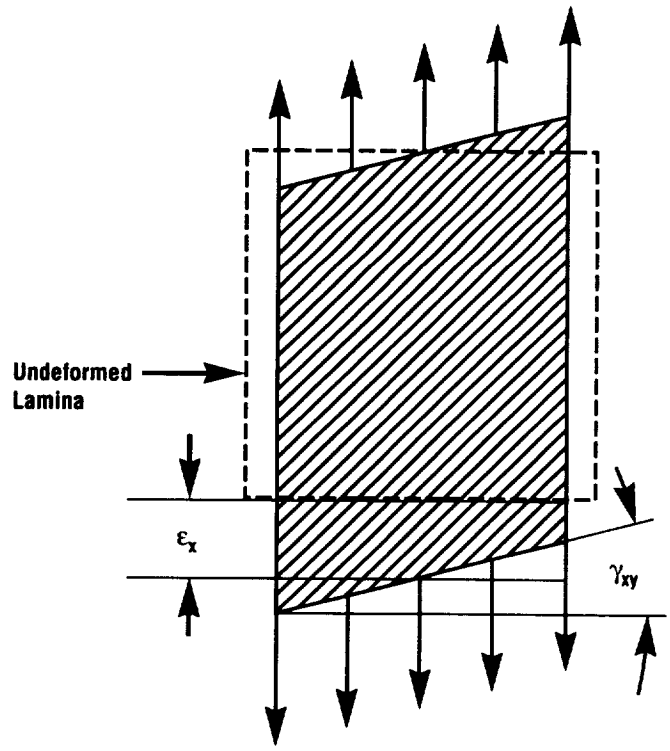

Figure A-1. Deformation of a 45° lamina subject to a uniform stress.

In actuality, the strain is uniform across the loading edges since the specimen is clamped at these boundaries. The stress/strain relationship is given by:

$$\begin{bmatrix}\sigma_x\\ \sigma_y\\ \tau_{xy}\end{bmatrix} = \begin{bmatrix}\overline{Q_{11}}\,\overline{Q_{12}}\,\overline{Q_{16}}\\ \overline{Q_{12}}\,\overline{Q_{22}}\,\overline{Q_{26}}\\ \overline{Q_{16}}\,\overline{Q_{26}}\,\overline{Q_{66}}\end{bmatrix}\begin{bmatrix}\varepsilon_x\\ \varepsilon_y\\ \gamma_{xy}\end{bmatrix}, \tag{A-6}$$

where,

$$\overline{Q_{11}} = Q_{11}\cos^4\theta + 2(Q_{12} + 2Q_{66})\cos^2\theta\sin^2\theta + Q_{22}\sin^4\theta,$$

$$\overline{Q_{12}} = (Q_{11} + Q_{22} - 4Q_{66})\cos^2\theta\sin^2\theta + Q_{12}(\cos^4\theta + \sin^4\theta),$$

$$\overline{Q_{22}} = Q_{11}\sin^4\theta + 2(Q_{12} + 2Q_{66})\cos^2\theta\sin^2\theta + Q_{22}\cos^4\theta,$$

$$\overline{Q_{16}} = (Q_{11} - Q_{12} - 2Q_{66})\cos^3\theta\sin\theta + (Q_{12} - Q_{22} + 2Q_{66})\cos\theta\sin^3\theta, \tag{A-7}$$

$$\overline{Q_{26}} = (Q_{11} - Q_{12} - 2Q_{66})\cos\theta\sin^3\theta + (Q_{12} - Q_{22} + 2Q_{66})\cos^3\theta\sin\theta,$$

$$\overline{Q_{66}} = (Q_{11} + Q_{22} - 2Q_{12} - 2Q_{66})\cos^2\theta\sin^2\theta + Q_{66}(\cos^4\theta + \sin^4\theta),$$

and the Q_{ij} are determined from the lamina engineering constants as:

$$Q_{11} = \frac{E_1}{1 - \upsilon_{12}\upsilon_{21}}, \qquad Q_{22} = \frac{E_2}{1 - \upsilon_{12}\upsilon_{21}},$$

$$Q_{12} = \frac{\upsilon_{21}E_1}{1 - \upsilon_{12}\upsilon_{21}}, \qquad Q_{66} = G_{12}. \tag{A-8}$$

Thus, for a uniform strain applied in the x-direction, equation (A-6) becomes:

$$\begin{bmatrix} \sigma_x \\ \sigma_y \\ \tau_{xy} \end{bmatrix} = \begin{bmatrix} \overline{Q_{11}}\ \overline{Q_{12}}\ \overline{Q_{16}} \\ \overline{Q_{12}}\ \overline{Q_{22}}\ \overline{Q_{26}} \\ \overline{Q_{16}}\ \overline{Q_{26}}\ \overline{Q_{66}} \end{bmatrix} \begin{bmatrix} \varepsilon_x \\ 0 \\ 0 \end{bmatrix}, \tag{A-9}$$

which, for shear stress, reduces to:

$$\tau_{xy} = \overline{Q_{16}}\varepsilon_x \tag{A-10}$$

where (from equation (A-7)),

$$\overline{Q_{16}} = (Q_{11} - Q_{12} - 2Q_{66})\cos^3\theta\sin\theta + (Q_{12} - Q_{22} + 2Q_{66})\cos\theta\sin^3\theta,$$

which is a maximum at $\theta = 45°$. Thus, to induce the maximum amount of shear stress into a lamina by applying only a uniform tensile strain, the fibers should be at 45° to the direction of pull. This is why a tensile coupon is pulled at 45° and –45° to the fibers in order to find a lamina's in-plane shear strength (both +45° and –45° plies must be included to give a symmetric laminate.)

From: Nettles, A.T., *Composite Processing Development to Improve Interlaminar Strength Using Ply Interface Particles (Center Director's Discretionary Fund Final Report No. 93-13),* NASA Technical Memorandum 108495, June 1995, pp. 3-6.

For additional information on the mechanics of composite materials see Nettles, A.T., *Basic Mechanics of Laminated Composite Plates,* NASA Reference Publication 1351, October 1994, pp. 1-11.

☆ U.S. GOVERNMENT PRINTING OFFICE—1996—532-128/40063

REPORT DOCUMENTATION PAGE

Form Approved
OMB No. 0704-0188

1. AGENCY USE ONLY (Leave Blank)	2. REPORT DATE	3. REPORT TYPE AND DATES COVERED
	November 1996	Technical Paper

4. TITLE AND SUBTITLE
Low-Temperature Mechanical Testing of Carbon-Fiber/Epoxy-Resin Composite Materials

5. FUNDING NUMBERS

6. AUTHOR(S)

A.T. Nettles and E.J. Biss

7. PERFORMING ORGANIZATION NAME(S) AND ADDRESS(ES)

George C. Marshall Space Flight Center
Marshall Space Flight Center, Alabama 35812

8. PERFORMING ORGANIZATON REPORT NUMBERS

M-821

9. SPONSORING/MONITORING AGENCY NAME(S) AND ADDRESS(ES)

National Aeronautics and Space Administration
Washington, DC 20546-0001

10. SPONSORING/MONITORING AGENCY REPORT NUMBER

NASA TP-3663

11. SUPPLEMENTARY NOTES

Prepared by Materials and Processes Laboratory, Science and Engineering Directorate.

12a. DISTRIBUTION/AVAILABILITY STATEMENT

Unclassified-Unlimited
Subject Category 24

12b. DISTRIBUTION CODE

13. ABSTRACT *(Maximum 200 words)*

The use of cryogenic fuels (liquid oxygen and liquid hydrogen) in current space transportation vehicles, in combination with the proposed use of composite materials in such applications, requires an understanding of how such materials behave at cryogenic temperatures. In this investigation, tensile intralaminar shear tests were performed at room, dry ice, and liquid nitrogen temperatures to evaluate the effect of temperature on the mechanical response of the IM7/8551-7 carbon-fiber/epoxy-resin system.

Quasi-isotropic lay-ups were also tested to represent a more realistic lay-up. It was found that the matrix became both increasingly resistant to microcracking and stiffer with decreasing temperature. A marginal increase in matrix shear strength with decreasing temperature was also observed. Temperature did not appear to affect the integrity of the fiber-matrix bond.

14. SUBJECT TERMS	15. NUMBER OF PAGES
composite materials, cryogenics	28
	16. PRICE CODE: A03

17. SECURITY CLASSIFICATION	18. SECURITY CLASSIFICATION OF THIS PAGE	19. SECURITY CLASSIFICATION OF ABSTRACT	20. LIMITATION OF ABSTRACT
Unclassified	Unclassified	Unclassified	Unlimited